# Thermal degradation, visco-elastic and fire-retardant behavior of hybrid *Cyrtostachys Renda*/kenaf fiber-reinforced MWCNT-modified phenolic composites

Tamil Moli Loganathan[1] · Mohamed Thariq Hameed Sultan[1,2,3] · Qumrul Ahsan[4] · Mohammad Jawaid[2] · Jesuarockiam Naveen[5] · Ain Umaira Md Shah[1] · Abd. Rahim Abu Talib[1] · Adi Azriff Basri[1]

## Abstract

Natural fibers have emerged as a potential alternate to synthetic fibers, because of their excellent performance, biodegradability, renewability and sustainability. This research has focused on investigating the thermal, visco-elastic and fire-retardant properties of different hybrid Cytostachys Renda (CR)/kenaf fiber (*K*) (50/0; 35/ 15, 25/25, 15/ 35, 0/50)-reinforced MWCNT (multi-walled carbon nanotubes)-modified phenolic composites. The mass% of MWCNT-modified phenolic resin was maintained 50 mass% including 0.5 mass% of MWCNT. In order to achieve homogeneous dispersion ball milling process was employed to incorporate the MWCNT into phenolic resin (powder). Thermal results from thermogravimetric analysis and differential scanning calorimetric analysis revealed that the hybrid composites (35/15; 35 mass% CR and 15 mass% *K*) showed higher thermal stability among the composite samples. Visco-elastic results revealed that kenaf fiber-based MWCNT-modified composites (0/50; 0 mass% CR and 50 mass% *K*) exhibited higher storage and loss modulus due to high modulus kenaf fiber. Fire-retardant analysis (UL-94) showed that all the composite samples met H-B self-extinguishing rating and exhibited slow burning rate according to limiting oxygen index (LOI) test. However, (15/35; 15 mass% CR and 35 mass% *K*) hybrid composites showed the highest time to ignition, highest fire performance index, lowest total heat release rate, average mass loss rate, average fire growth rate index and maximum average rate of heat emission. Moreover, the smoke density of all hybrid composites was found to be less than 200 which meets the federal aviation regulations (FAR) 25.853d standard. Technique for Order Preference by Similarity to Ideal Solution (TOPSIS) was carried out to select an optimal composite sample considering the thermal, visco-elastic and fire-retardant behaviors. Through TOPSIS analysis, the hybrid (15/35; 15 mass% CR and 35 mass% K) composite sample has been selected as an optimal composite which can be used for high-temperature aircraft and automotive applications.

**Keywords** *Cytostachys Renda* · Kenaf fiber · Multi-walled carbon nanotubes · Modified phenolic · Thermal properties · TOPSIS

✉ Mohamed Thariq Hameed Sultan
thariq@upm.edu.my

1 Department of Aerospace Engineering, Faculty of Engineering, Universiti Putra Malaysia, 43400 UPM Serdang, Selangor Darul Ehsan, Malaysia

2 Laboratory of Biocomposite Technology, Institute of Tropical Forestry and Forest Products (INTROP), Universiti Putra Malaysia, 43400 UPM Serdang, Selangor Darul Ehsan, Malaysia

3 Aerospace Malaysia Innovation Centre (944751-A), Prime Minister's Department, MIGHT Partnership Hub, Jalan Impact, 63000 Cyberjaya, Selangor Darul Ehsan, Malaysia

4 University of Asia Pacific, 74/A Green Road, 1205 Dhaka, Bangladesh

5 School of Mechanical Engineering, Vellore Institute of Technology, Vellore 632014, India

## Introduction

Synthetic fibers have profound impact on the environment and waste management problems. The prohibition on composite landfills, led by the evacuation of aircrafts owing to the COVID-19 pandemic, is greatly stimulating the adoption of a sustainability and recycling strategy. The exploration of bio-composites generated from bio-based fibers and matrix developed from agricultural waste continues to expand in an effort to replace traditional fossil-based composites [1–3]. In comparison with synthetic fiber-based composites, natural or bio-based fiber composites are renewable, sustainable, exhibit low environmental impact and can be utilized in numerous applications [4].

*Cyrtostachys renda* (CR) is a plant from the palm family that has a physical resemblance to *Areca catechu.* CR is known to be an alternative plant fiber used as reinforcement in polymeric composites to add value to agro-waste materials. It has been experimentally observed in a previous study that CR fibers are found to be compatible with phenolic resin to improve mechanical properties [5]. Kenaf fiber, known as *Hibiscus cannabinus L.* in its scientific name, belonging to the *Malvaceace* family is a form of bast fiber. It has the desirable characteristics of high toughness, strength and stiffness that could possibly be used as a fiber reinforcement to reinforce polymers at high aspect ratios [6]. Kenaf fiber offers a high-performance composite with great mechanical strength and thermal stability. Also, it has demonstrated excellent compatibility with phenolic matrix [7]. The findings from previous studies indicated that the combination of palm fiber and kenaf compensates each other on tensile and impact characteristics to produce a hybrid composite with increased mechanical characteristics [8, 9]. The kenaf bast fiber is used due to its high tensile strength and the oil palm fiber due to its high toughness and high thermal stability. The hybrid composites can surpass the limitations of individual constituents. Development of these hybrid composites may be tailored to meet the required properties suitable for automotive and aviation industries.

Among different chemical treatments, alkali treatment is a simple and efficient surface modification technique to enhance the mechanical and thermal stability of natural fibers. The highest hemicellulose content removal was found in 3% of NaOH-treated fibers over 1 h of immersion time, compared to other parameters that were investigated by Loganathan et al. [5], and found that the major degradation shifted from 297 to 316 °C. Additionally, the final degradation shifted from 364 to 480 °C with an increase in char residue from 11.41 to 26.22%, compared to raw CR fiber. On the other hand, Abdullah et al. identified that the major degradation 3% of NaOH-treated kenaf fiber for an hour

occurred at 297 °C, and the final degradation at 358 °C with char residue of 15.78% [10]. Compared to raw kenaf fiber, the thermal stability of NaOH-treated kenaf fiber improved, likely due to the removal of non-cellulosic substances, especially hemicellulose. Based on this, the thermal stability values of NaOH-treated CR and kenaf fibers are better in their major and final degradation temperatures, with a comparison of jute (260 °C, 340 °C), sisal (250 °C, 345 °C) and cotton (265 °C, 330 °C) [11, 12].

Phenolic resin is a highly cross-linked thermoset polymer. It has the most fire resistance and thermal stability by char formation [13, 14]. Bio-phenolics were used in this research from cardanol-based resins extracted from cashew nut shell liquid (CNSL), classified as the novolac type. The limiting oxygen index (LOI) of phenolic resin is 25 which can be attributed to its slow burning rate [15]. This property makes phenolic as a promising matrix in automotive and aircraft structures at elevated temperatures. The integration of nanoparticles into polymers has demonstrated enhancement in various properties. Nanofillers including nanotube carbon (CNT), graphene fillers and nanoclays are often used to enhance fire resistance and thermal stability [16].

Asim et. al [17] investigated the characteristics of kenaf-reinforced phenolic composites, and thermogravimetric analysis revealed that pure phenolic was more stable, rather than kenaf fiber, while treated 50% kenaf composite increased the storage modulus, due to the fiber stiffness. Vertical and horizontal UL-94 tests proved that pure phenolic is extremely fire resistant, but kenaf fiber demonstrated greater fire resistance than pineapple fiber [17]. Asim et al. [14] also reported that 50% date palm fiber improved the storage modulus of phenolic composites due to suitable proportion and adhesions between fiber and matrix, while exhibited the highest stiffness. For thermal resistant applications, the higher lignin content of date palm fiber is suitable as a reinforcement fiber. The hybridization of pineapple (P) and kenaf (*K*)-reinforced phenolic composites on visco-elastic properties was investigated by researchers [18]. It was found that the highest storage, loss modulus and lowest burning rates were obtained from treated fibers P:K ratio of 7:3 compared to untreated fibers. The proportion of P:K at 3:7, the thermally stable and slowest burning rate in UL 94, and also the result of thermogravimetric analysis (TGA) indicate that the treated hybrid composites have a greater glass transition compared to untreated hybrid composites [18].

Phenolic resin is renowned for its inherent fire resistance. Nevertheless, it exhibits relatively low mechanical strength and brittleness. Therefore, low content of MWCNT as inorganic nanoparticles is used as a modifier to toughen the phenolic composites. In a previous study, it was reported that dry mixing dispersion of MWCNT in novolac-type phenolic resin after 25 h of ball milling exhibited a significant improvement in flexural strength

compared to wet mixing dispersion [19]. Eslami et al. stated that the flexural strength and thermal stability of phenolic composites increase with the rise in MWCNT up to 0.5 mass% [20]. The addition of nanoparticles such as MWCNT further improves the thermal resistance of polymeric matrix. As soon as the pyrolysis reaction began, nanoparticles formed an extremely viscous melting layer and covered the residual char. Char is represented as an antioxidant and a thermal protection barrier in developing a carbon-based network. The addition of MWCNT resulted in the re-emission of large amounts of incident radiation to the gas phase in the charcoal residues, which lowered the amount of heat transmitted to the inner virgin material and decreased the pyrolysis rate [21]. To date, studies have been performed to investigate the thermal effects of MWCNT on phenolic composites [22, 23] and thermal properties of natural fibers as well as hybrid fibers on phenolic composites [14, 17, 18].

This research has focused on investigating the thermal properties, especially the visco-elastic and fire-retardant behaviors of different proportions of hybrid Cytostachys Renda (CR)/kenaf fiber (K) (10C:0 K, 7C:3 K, 5C:5 K, 3C:7 K, 0C:10 K)-reinforced 0.5 mass% MWCNT-modified phenolic composites. Hybridizing CR and K fiber in a MWCNT-modified phenolic matrix would take the advantage of individual constituents and provide superior properties compared to synthetic fiber-based polymeric composites. Moreover, this multiscale hybrid composites can be an alternative to synthetic fiber-reinforced polymeric composite. In our previous study, the authors investigated the physical and mechanical properties of hybrid Cytostachys Renda (CR)/kenaf fiber (*K*)-reinforced MWCNT-phenolic composites [24]. To date, no study has been reported to examine the thermal properties of the integration of hybrid natural fibers into MWCNT-phenolic composites. This research was therefore mainly carried out to fill the gap by studying the thermal effects of hybridization of CR and kenaf in modified MWCNT-phenolic composites. In addition, this study has been implemented with the aim of using hybrid bio-composites with natural fibers (CR and kenaf) as reinforcement as well as a renewable material for the transport industry, in particular the automobile and aeronautical industries, to satisfy the Federal Motor Vehicle Safety Standard (FMVSS) and Federal Aviation Administration (FAA) specifications.

# Materials and method

## Materials

The physical and mechanical properties of *Cytostachys Renda* (CR) and kenaf fiber are described in a literature [24]. R&M Chemicals supplied sodium hydroxide pellets with a molecular mass of 40 g mol$^{-1}$ and a density of 2.13 g cm$^{-3}$, and CR fibers were extracted manually from the leaf stalk using the retting technique and obtained from the Telok Panglima Garang plantation in Malaysia. Kenaf fiber and MWCNT were purchased from ZKK Sdn Bhd, Malaysia. MWCNT was synthesized using a chemical vapor deposition (CVD) technique consisting of 8–15 nanotube layers with a diameter range of 12–15 nm, a size range of 3–15 µm and a purity exceeding 97%. Chemovate Girinagar in Bangalore, India, supplied the phenolic resin (Novolac type) derived from cashew nut shell liquid (CNSL) mixed with a 10% hexamine hardener.

## Preparation of CR and Kenaf fiber

Dry CR fiber and kenaf fiber were ground, pulverized and sieved using a sieve shaker with a size of < 0.3 mm. The fibers were immersed in 100 mL of distilled water at concentrations of 3 mass% of NaOH for 1 h. They were then rinsed multiple times with distilled water to eliminate any residue and dried for 24 h in an air circulation oven set to 80 °C.

## Fabrication of composites

0.5 mass% of MWCNT was added to the phenolic resin, and the contents were mixed and milled using a dry ball for a total of 25 h to produce a homogeneous distribution. The CR and/or kenaf hybrid composites with the composition in Table 1 were produced by a hand-lay-up technique with a mold size of 150 mm × 150 mm × 3 mm. The details of the hybrid composite preparation was described in the previous study [24].

**Table 1** Formulation of hybrid composites

| Designation ratio of hybrid composites | 0.5 mass% MWCNT + Phenolic resin / mass% | CR / mass% | K / mass% |
|---|---|---|---|
| 10C:0 K | 50 | 50 | 0 |
| 7C:3 K | 50 | 35 | 15 |
| 5C:5 K | 50 | 25 | 25 |
| 3C:7 K | 50 | 15 | 35 |
| 0C:10 K | 50 | 0 | 50 |

C Cyrtostachys renda, K Kenaf

## Characterization

### Thermal properties

#### Thermogravimetric Analysis (TGA)

Thermal stability of CR and/or Kenaf composite and hybrid composite samples were characterized using a Mettler Toledo Thermogravimetric Analyzer-Differential Scanning Analysis (TGA–DSC) (Model: TGA–DSC HT 3) according to ASTM1131. The analysis was executed in a nitrogen environment at a flow rate of 50 mL min$^{-1}$ and a temperature range of 25–900 °C at a heating rate of 10 °C min$^{-1}$.

#### Differential scanning calorimetry (DSC)

DSC testing was performed using a Mettler Toledo Thermogravimetric Analyzer-Differential Scanning Analysis (TGA–DSC) (Model: TGA–DSC HT 3) according to ASTM D 3418. The analysis was conducted using a nitrogen purge at a flow rate of 50 mL min$^{-1}$ and a heating rate of 10 °C min$^{-1}$ across a temperature range of 25–900 °C.

### Visco-elastic properties

Dynamic mechanical analysis (DMA) was performed to study the visco-elastic performance of polymer composites of hybrid CR/K/phenolic composites using Perkin Elmer (DMA 8000) instrument. DMA was carried out as per ASTMD 4065 with dimensions of 60 mm × 10 mm × 3 mm, functional in a three-point bending method. The specimens were subjected to sinusoidal strain at a frequency of 0.5 Hz. The specimens were heated at a rate of 5 °C min$^{-1}$ from ambient temperature to 150 °C.

### Flammability properties

The flammability properties of loading of CR fiber-reinforced MWCNT-phenolic composites were measured using Underwriters Laboratories (UL 94), limiting oxygen index (LOI), cone calorimetry and smoke density.

#### Underwriters laboratories 94 horizontal burning test (UL 94HB)

UL 94 examines the plastic material's ability to extinguish a fire after ignition and its dripping behavior under controlled environments. A horizontal burning test was used to determine the flammability of phenolic composites in accordance with ASTM D 635 to measure burning rate and burning time using UL94 supplied by Festec International Co, Ltd,

Korea. Five identical samples for each set with dimensions of 125 mm × 13 mm × 3 mm were produced. The length side was marked 25 mm from each edge. For the horizontal UL-94 test, the specimen was positioned horizontally and one end was exposed to a flame. The time taken for the flame to travel from 25 to 100 mm (from the end) was recorded. The composites' burning rates are then determined using Eq. 1.

$$\text{Burning velocity, V} = 60 \, L/t \tag{1}$$

where $V$ denotes the burning velocity rates (mm min$^{-1}$), $L$ represents the burnt length (mm), and t is the burning period (s).

#### Limiting oxygen index (LOI)

The limiting oxygen index (LOI) is the lowest oxygen concentration for burning represented as a volume %. The LOI test was performed in accordance with ASTM D 2863 supplied by Festec International Co, Ltd, Korea. Ten replicate samples with dimensions of 100 mm × 6.5 mm × 3 mm were produced for each set. The specimen was clamped vertically in the sample holder and allowed to burn for 10 s at a time until the flames were initiated. LOI value calculated by following Eq. (2):

$$LOI(vol.\%) = C_F + kd \tag{2}$$

where $C_F$ signifies the final value of oxygen concentration in vol.% for the previous five measurements, $d$ represents the interval difference in vol.% between oxygen concentration levels (0.2 vol.%), and $k$ denotes a factor derived from the experimental value.

#### Cone calorimetry test

A cone calorimeter measures the heat release rate (HRR), peak heat release rate (pHRR), total heat release rate (THR), time to ignition (TTI), smoke production rate, mass loss rate (MLR) and generation of carbon monoxide and carbon dioxide when specimens are exposed to conical heater resources. This test is conducted in accordance with ISO 5660 using a FESTEC International, Korea cone calorimeter supplied by Fire Engineering & Science Technology. The specimens were prepared to be 100 mm × 100 mm × 3 mm in size. The specimens were covered in aluminum foil on the side and bottom, then put horizontally on the sample holder and subjected to a 35 kW m$^{-2}$ heat flux irradiation.

#### Smoke density test

Smoke density is evaluated by detecting the smoke density of the static smoke produced when the volume

of radiant heat is exposed to the flat side of the specimen. This accurately determines the optical intensity of smoke and any toxic gas emitted by the material when it is exposed to the source of the fire. The optical smoke density was calculated using the smoke density tester supplied by FESTEC International, Korea (SB501) in compliance with ASTM E662. The dimensions of the specimen were 75 mm × 75 mm × 3 mm. The specimen was coated in aluminum foil of 0.04 mm thickness and exposed to a heat flux of 25 kW m2$^{-1}$ in non-flammable test mode. The ray of light reflected through the chamber. Eventually, the smoke intensity was calculated by the measurement of the obscuring of the light beam using a photosensor. The optical device permitted the continuous calculation of the optical smoke density (Ds) and the parameter VOF 4. The latter is based on the Ds curve, informs how much smoke is formed during the first 4 min of fire and was calculated according to Eq. 3.

$$\text{VOF } 4 \; = \; \tfrac{1}{4}\,SD_1\min + SD_2\min + SD_3\min + \left(SD_4\min/2\right) \tag{3}$$

where $SD_1$ min, $SD_2$ min, $SD_3$ min and $SD_4$ min are the specific optical densities observed at the first, second, third and fourth minutes, respectively.

## Technique for order preference by similarity to the ideal solution (TOPSIS)

The Technique for Order Preference by Similarity to the Ideal Solution (TOPSIS) technique is a Multi-Criterial Decision Making (MCDM) approach that was used to identify an ideal hybrid ratio for thermal characteristics between CR and kenaf fiber-reinforced modified phenolic composites. The TOPSIS technique considers both the degree of distance of each alternative from positive and negative ideals. As indicated in Table 2, there are 5 criteria and 5 alternatives in this study; these are ranked based on the TOPSIS method. The following criteria and the weightage (based on importance) for the selection are made according to the composite application. + sign indicates that higher numerical value exhibits superior performance, whereas − sign reveals that lower numerical

**Table 2** Characteristics of Criteria

| Alternative | Criteria | Type | Mass |
| --- | --- | --- | --- |
| 10C:0 K | TGA | + | 0.2 |
| 7C:3 K | Storage Modulus | + | 0.2 |
| 5C:5 K | LOI | + | 0.2 |
| 3C:7 K | FPI | + | 0.2 |
| 0C:10 K | VOF | − | 0.2 |

value exhibits higher performance. The TOPSIS method calculation is described in the literature [24].

## Results and discussion

### Thermal properties

#### Thermogravimetric analyzer (TGA)

TGA and DTG graph of CR and K composites and hybrid composites are shown in Fig. 1. All the TGA curves showed similar tendencies. TGA findings are presented in Table 3 for CR and K fiber-reinforced MWCNT-phenolic composite. Increased absorption of moisture was found in all natural fiber composites, with mass loss ranging from 5.3 to 6.15%. For C and K composites and hybrid composites, the first mass loss or **initial degradation** of 25–160 °C refers to the vaporization of water molecules of composite samples. The second level of degradation or known as major degradation could be found above 150 °C owing to the decomposition of chemical compositions present in CR. Kenaf fibers are decomposed at the following temperatures, cellulose: 275–500 °C, hemicellulose: 150–350 °C and lignin 250–500 °C [25]. In addition, above 500 °C, decomposition of the aromatic phenolic occurred, which are low molecular mass such as benzene, phenols and toluene [26]. The third step of deterioration is known as final degradation; it begins beyond 500 °C and correlates with a polycyclic aromatic ring of phenolic and MWCNT. The peak also implies the reactions of polyaromatic reactions as phenolic resin is processed at a temperature of more than 750 °C, resulting in a progressive conversion to amorphous carbon [27]. **In addition,** it was reported that the raw MWCNT oxidation began at 420 °C and ended at 630 °C [28]. **Based on the TGA and DTG curves**, there is not much significant difference with various proportions of hybridization of CR and kenaf composites. Pristine phenolic reported that the degradation temperature starts at 420.73 °C, and the residual residues in pristine phenolic were 55.97% [7], indicating the highest thermal stability relative to natural hybrid phenolic composites. Figure 2 represents the graphical illustration of the thermal degradation pathway of CR/kenaf-reinforced MWCNT-phenolic hybrid composites.

#### Differential scanning analysis (DSC)

Figure 3 demonstrates the DSC plots of hybridization of C and kenaf-reinforced MWCNT-phenolic composites. During the DSC testing, the heat flow was calculated as a function of time and temperature to determine the glass transition temperature ($T_g$), temperature of curing and decomposition [29]. The DSC curves of all composite samples follow a

**Fig. 1** TGA and DTG curve of hybrid CR and Kenaf reinforced phenolic composites
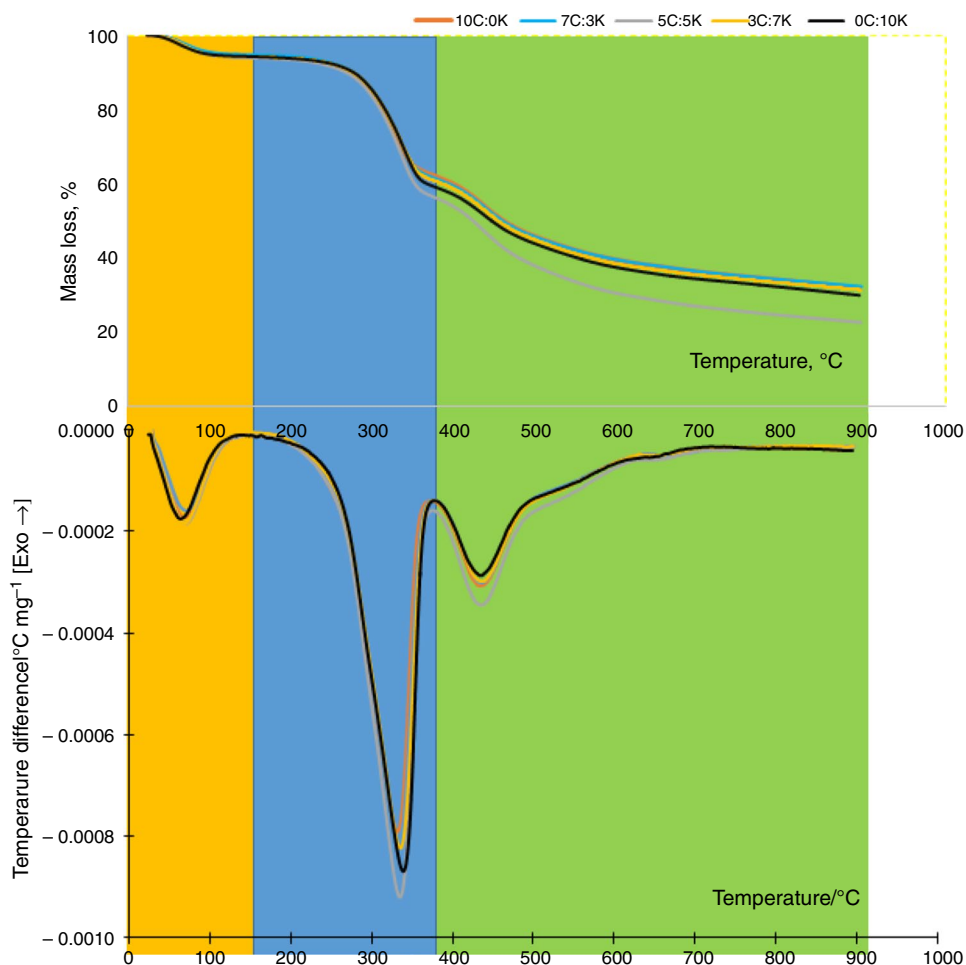


**Table 3** Profiles of decomposition of hybrid composites in nitrogen environment

| Composites | Temperature range / °C | Peak Temperature / °C | Mass loss / % | Residue / % | Ref. |
|---|---|---|---|---|---|
| 10C:0 K | 25–160 | 68 | 5.80 | 32.07 | Present study |
|  | 160–373 | 331 | 31.98 |  |  |
|  | 373–763 | 434 | 21.31 |  |  |
| 7C:3 K | 25–147 | 71 | 5.30 | 32.46 |  |
|  | 147–377 | 333 | 33.33 |  |  |
|  | 377–822 | 436 | 23.26 |  |  |
| 5C:5 K | 25–148 | 70 | 6.15 | 22.80 |  |
|  | 147–374 | 335 | 37.45 |  |  |
|  | 374–833 | 434 | 32.38 |  |  |
| 3C:7 K | 25–151 | 69 | 6.15 | 31.59 |  |
|  | 151–377 | 335 | 37.45 |  |  |
|  | 377–803 | 436 | 32.38 |  |  |
| 0C:10 K | 25–150 | 63 | 5.71 | 30.09 |  |
|  | 150–377 | 339 | 37.45 |  |  |
|  | 377–717 | 434 | 32.38 |  |  |
| Pristine phenolic | 420–600 | 510 | 32.16 | 55.97 | [6] |

Thermal degradation, visco-elastic and fire-retardant behavior of hybrid *Cyrtostachys*...

14085

**Fig. 2** Graphical represents of the thermal degradation pathway of CR/Kenaf reinforced MWCNT-phenolic hybrid composites
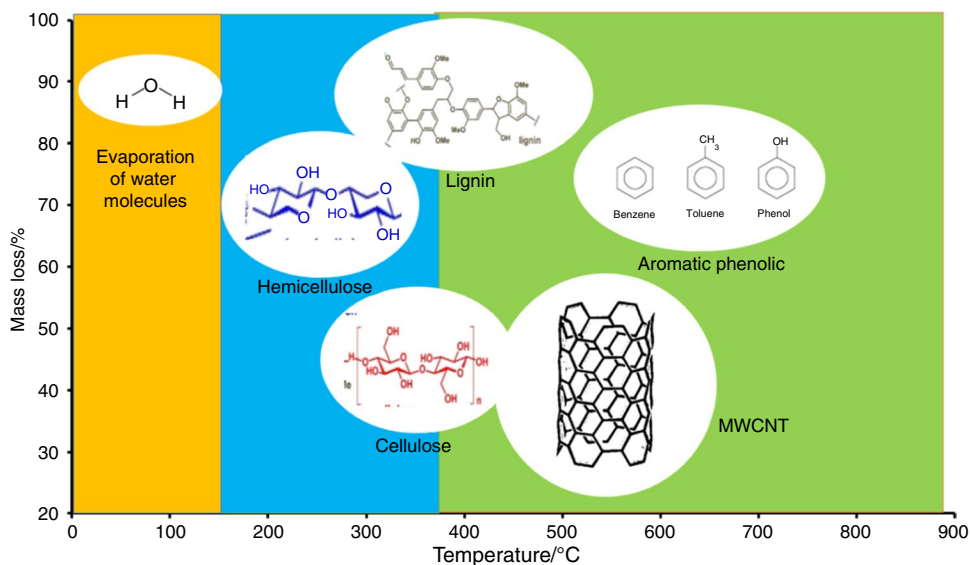
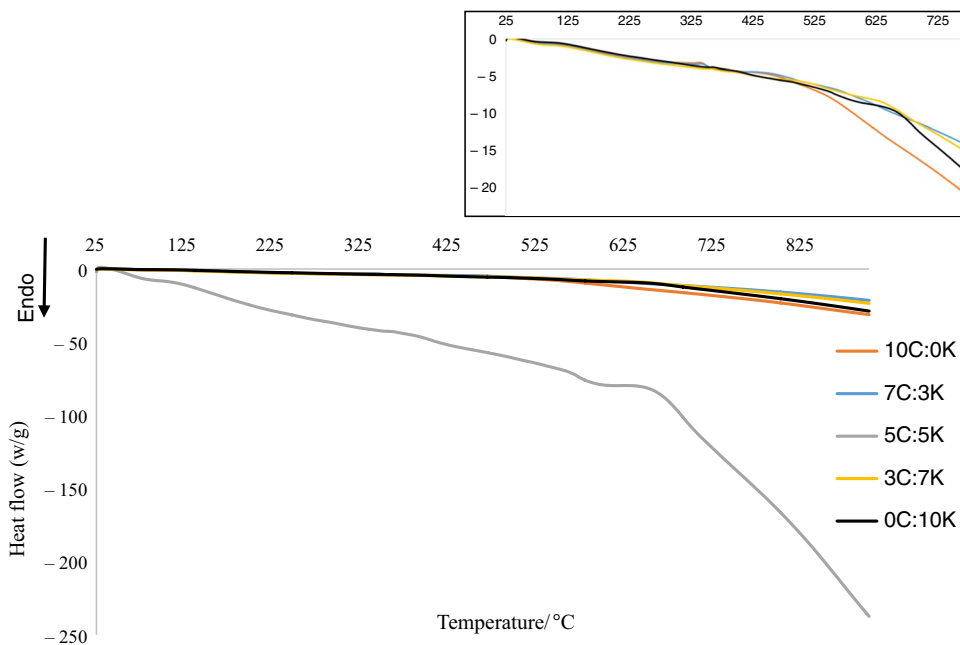

**Fig. 3** DSC graph of hybrid composites



**Table 4** Result obained from DSC graph

|  | Onset temp | Peak temp | Offset Temp | Latent heat/ J g$^{-1}$ | Residue |
|---|---|---|---|---|---|
| 10C:0 K | 325 | 341 | 357 | 40.19 | 32.07 |
| 7C:3 K | 323 | 343 | 363 | 88.83 | 32.46 |
| 5C:5 K | 358 | 365 | 372 | 7.84 | 22.80 |
| 3C:7 K | 348 | 359 | 378 | 11.91 | 31.59 |
| 0C:10 K | 347 | 356 | 362 | 10.78 | 30.09 |

similar pattern, as shown in Fig. 3. All of the composites endured direct decomposition due to phenolic as the thermoset polymeric matrix. As a consequence, the thermoset polymer's degree of crystallinity was not detected. No exothermic peak was observed disproving the complete cure of all the composites. The first energy peak is the endotherm phase found at 330–360 °C, which indicates the primary evaporation of a portion of the composite material. It was ascribed to the deterioration of hemicellulose, cellulose and lignin as the major constituents of CR and kenaf fiber. The final endothermic transformation happens above 435 °C and is attributable to aromatic phenolic and MWCNT decomposition. DSC results were similar to TGA and DTA results. Based on the char residue of DSC in Table 4, 7C:3 K composites have been chosen as efficient hybrid composites in terms of thermal stability.

## Visco-elastic properties

DMA is a valuable technique for determining the viscoelastic characteristics of cross-linking materials during initial relaxation. It measures as a function of temperature and frequency as deformed by sinusoidal displacement [30]. In DMA, storage modulus ($E'$) is an assessment of its stored energy during a period under load as an elasticity of a materials, loss modulus ($E''$) refers to a plasticity of a materials and measure dissipated energy in terms of heat, while loss factor, Tan $\delta$ (E′/E′), is related to molecular motion or internal friction of energy dissipation [31].

### Storage modulus (E′)

Storage modulus curve provided information regarding the degree of cross-linking, stiffness, rigidity and behavior of the materials' fiber/matrix interfacial bonding. The storage modulus was categorized into three regions such as glassy state, transition region and rubbery plateau state, as shown in Fig. 4. Due to the closely packed molecules, very high storage modulus value composite structure is very stiff and rigid in a glassy region, ascribed to rigid polymeric chain. The glass transition region, E′, was found to be lowered above Tg in the second stage owing to polymer chain movement. As a result, the mobility of the polymeric chain influences not only the stability but also the fiber/matrix adhesion [32]. However, the mobility of the polymeric chain accelerated at a higher temperature in the third level, rubbery plateau region [33].

Figure 4a displays the storage modulus by effect of temperature on CR, *K* and hybrid composites with relative mass ratio of CR:K fibers (7:3, 5:5, 3:7). The *C* composite and hybrid composites' storage modulus values were identical at low temperatures. The *K* composite, on the other hand, had a higher storage modulus value. However, no significant

difference was found in the rubbery region since the mobility of the polymeric chain increased significantly with temperature due to the loss of the closely packed molecular structure. Asim et al. reported the same finding that *K* fiber was closely packed with phenolic matrix and did not allow for mobility of molecular structure [7]. This is attributed to the fact that kenaf fiber has a higher elasticity modulus (Young's modulus) than palm fibers [34]. It is also supported that the higher content of cellulose (72%) in *K* fiber, possesses a stronger interfacial bonding with phenolic resin as compared to cellulose content in CR fiber of 45.2% [5]. The incorporation of *K* fiber in phenolic resin is illustrated in Fig. 5.

Table 5 shows the storage modulus at the initial glassy (30 °C) to transition region (120 °C) and found that the hybrid composites values lie in between border of CR composites and *K* composites, except for 5CR:5 K composites. The addition of stiff fiber as *K* to the C/phenolic composites improved the storage modulus significantly. The addition of K in CR composites (7C:3 K) showed better storage modulus in comparison with CR composites. Compared to the other composites, 3CR:7 K and 5CR:5 K hybrid composites display lower modules in both glassy and rubbery phases, indicating that they are more flexible with lower stiffness [12]. In addition, the trends of graph hybrid composites 7CR:3 K and 10CR:0 K show that they are hard and rigid, while 3CR:7 K and 5CR:5 K are stiff and soft because of incompatibility between the mass fraction between CR and *K* fibers. The $E'$ value increases with the addition of kenaf fiber into CR composites, due to the hybrid effect of kenaf fiber, which increases the stiffness and rigidity of the composites. According to Jawaid et al., the $E'$ value is proportional to the interfacial strength. In comparison with CR composite, the results revealed that kenaf composite and hybrid composites have greater interface bonding. Based on Table 5, the fiber-reinforced phenolic improved the storage modulus with respect to the pristine phenolic composite. The pristine phenolic displays the lowest storage modulus owing to the enhanced molecular movement of the polymer chains above $T_g$ [35].

### Loss modulus, (E")

Loss modulus, *E*, is a property of the heat energy dissipated per temperature for visco-elastic material in a sinusoidal cycle. The curve of loss modulus CR, *K* and hybridization between CR and *K* with variation in mass fraction is presented in Fig. 4b. It has been observed that the $E'$ value increases for all composite specimens, reaches a plateau and then declines. The highest $E''$ was observed for 0C:10 K, followed by 7C:3 K, 10C:0 K, 3C:7 K and 5C:5 K composites as ranking. Previous researchers [7] have also found the same finding that 50% of NaOH-treated kenaf provided the highest loss modulus among the other hybrid composites.
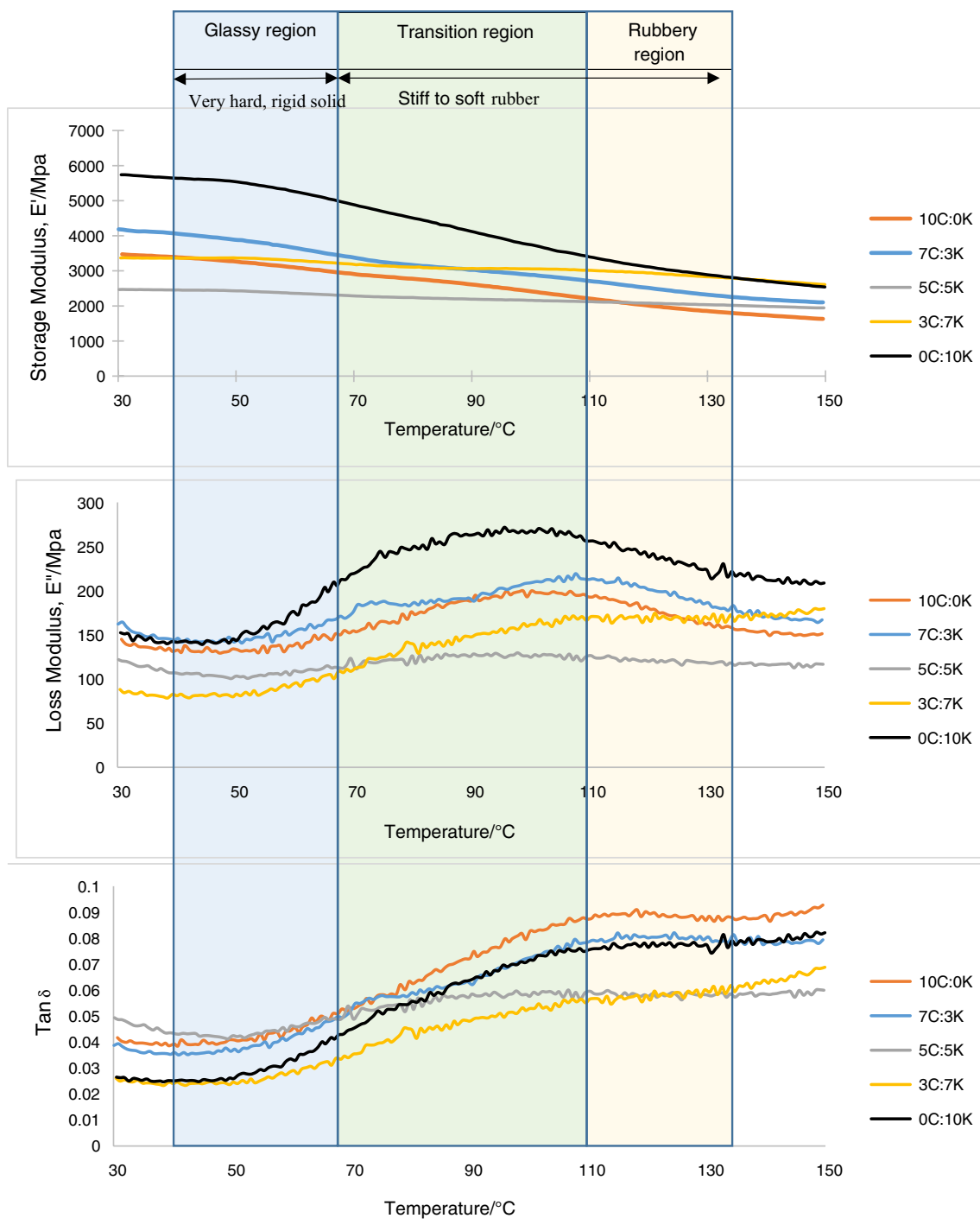
**Fig. 4** Results of DMA a) Storage Modulus, b) Loss Modulus, c) Tan δ

It is proven that 0C:10 K composites dissipated the highest heat energy per cycle during the deformation. The broadened peaks demonstrated the three-dimensional complexity of the chain polymer segment [36]. The addition of *K* fiber to C/phenolic composites contributes to broadening modulus peak due inhibition of the relaxation mechanism within the composites [12, 37]. There is change in the peaks of *E″* with variation in the mass proportion of hybridization between two fibers. The slippage between two fibers is resisted at low temperatures owing to the difference in the thermal expansion coefficient of matrix and fibers [38]. The slippage of fiber–fiber and fiber–matrix dissipated more
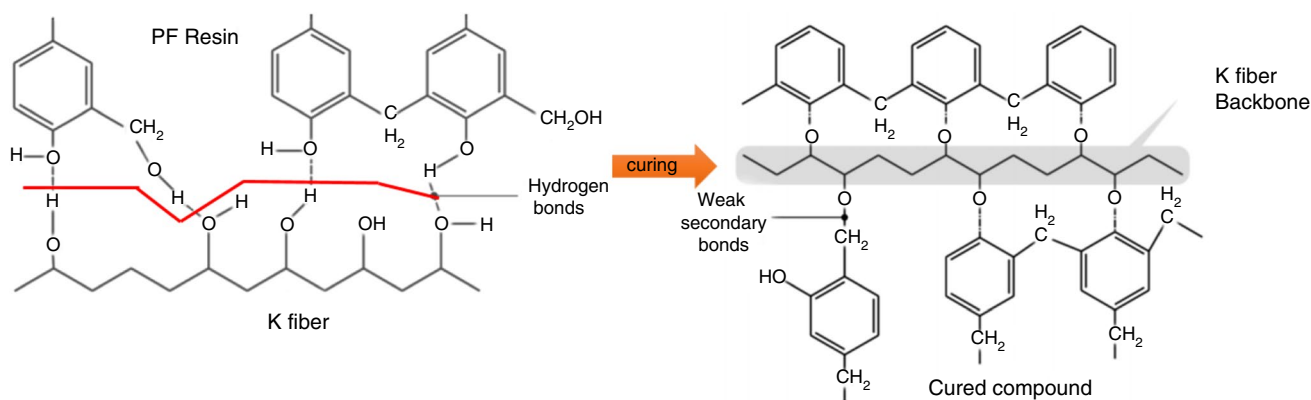
**Fig. 5** Chemical bonding of natural fiber with phenolic resin adapted from [35]

**Table 5** Results of DMA analysis on CR, K, and hybrid composites

| Specimens | Storage Modulus, E′ at 30 °C/MPa | Storage Modulus, E′ at 120 °C/MPa | Storage modulus Tg value/°C | Loss modulus Tg value/°C | Tan δ Tg value/°C | Ref. |
|---|---|---|---|---|---|---|
| 10C:0 K | 3470 | 2060 | 46.5 | 96.2 | 110 | Present study |
| 7C:3 K | 4180 | 2460 | 56.9 | 109.0 | 116 | Present study |
| 5C:5 K | 2470 | 2070 | 40.9 | 86.3 | 85 | Present study |
| 3C:7 K | 3370 | 3070 | 48.7 | 107 | 103 | Present study |
| 0C:10 K | 5740 | 3120 | 51.1 | 101 | 115 | Present study |
| Pristine phenolic | 2400 | 1250 | 68.89 | 93.01 | 80 | [6] |

heat. The high peak value of $E''$ indicates depletion of the intermolecular bonding [36]. The peak of the loss modulus and tan delta curve denoted the glass temperature, $T_g$ [39]. It was mentioned that loss modulus $T_g$ values were more practical compared to damping factor values [2]. The $T_g$ obtained from the loss modulus was found to be smaller than Tan $\delta$. It is important to identify the range of temperature where a material softens. The $T_g$ of all specimens fell in the range of temperature between 86 °C and 114 °C as shown in Table 5. 7C:3 K hybrid composites exhibited the highest $T_g$, while 5C:5 K showed the lowest $T_g$, among other tested composite materials. The high Tg values were associated with significant reductions in matrix molecular mobility when fiber was added, demonstrating a strong interfacial interaction between fiber and matrix [40]; the internal friction between fiber and matrix led to the dissipation of energy [41].

**Tan delta (Tan δ)**

Figure 4c displays the curve of Tan $\delta$ for the hybridization of CR-K fibers at various proportions of reinforced phenolic composites, as a function of temperature at a 0.5 Hz frequency. The damping factor was mainly influenced by fiber, matrix, fiber–matrix interfacial bonding and also the void content [39, 42]. $T_g$ value obtained from Tan $\delta$ curve

is tabulated in Table 5. It was noticed that $T_g$ value of $C$ composite and $K$ composite is 110 °C and 115 °C; however, the $T_g$ value of 7C:3 K composites improved to 116 °C. The transition of $T_g$ toward a higher temperature is associated with the decreased movement of molecular chains, which indicates that improved interfacial adhesion between the matrix and fibers at respective proportion of hybrid fibers reinforcement [40]. In Tan $\delta$ curve, lower damping values indicate enhanced interfacial adhesion, while higher Tan $\delta$ values imply a lack of interfacial interaction. 5C:5 K composite shows that a higher damping is the weakest interfacial adhesion of hybridization proportion, while $K$ composite is the lowest damping with a stronger interfacial bonding with the matrix. The curve of 7C:3 K composites lies in between K composite and C composite. In hybrid composites, the dispersion of the fibers would be greater than individual fiber composites. In addition, wetting stress and physical adhesion between the fiber matrix also increases for hybrid composites [43]. Interestingly, the compatible strain of the two hybrid fibers, positive effect could be observed in 7C:3 K composites.

**Fig. 6** Cole–Cole plots of the C, K and hybrid composites
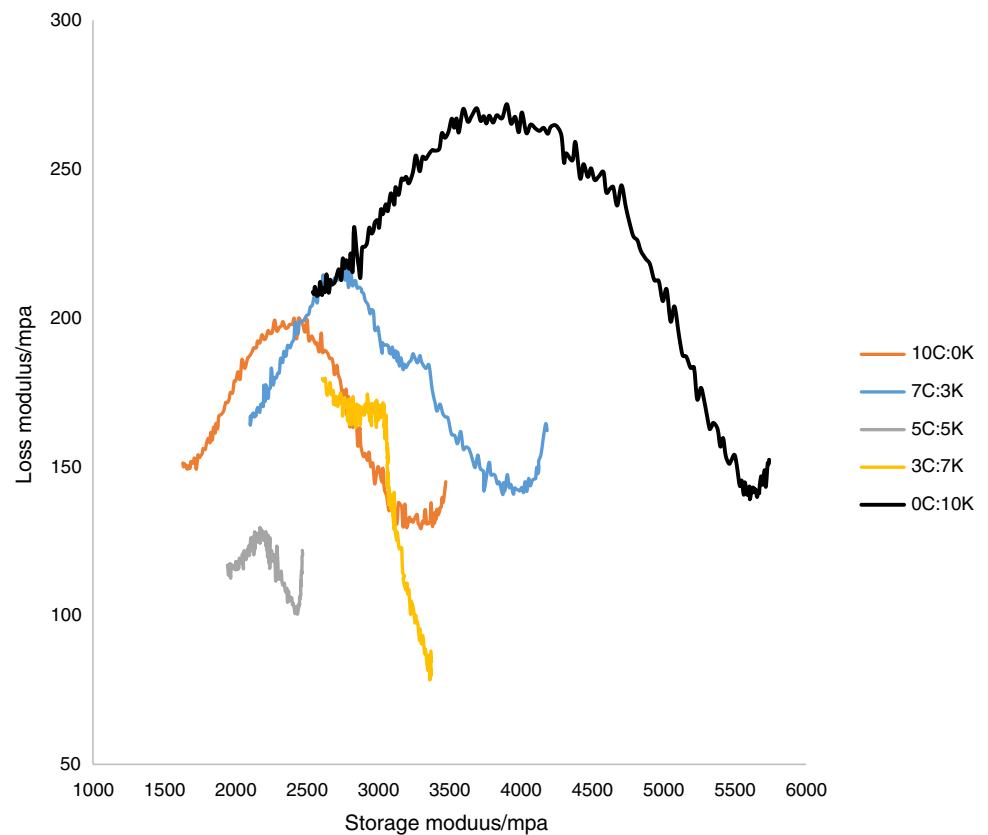


## Cole–cole plot

Cole–Cole plot represents the relationship between the loss modulus E″ and the storage modulus E′. Figure 6 displays the Cole–Cole plot of CR, *K* and hybrid composites. The Cole–Cole plot provides an extended information on homogeneity and structural modifications of the polymeric composites, resulting due to addition of fibers by mass fraction in proportion. According to a prior study, the smooth and semi-circular arc obtained from the Cole–Cole plot depicts a homogenous polymeric system with a well-dispersed filler [2]. On the other hand, irregular or defective semicircular curves indicate a polymeric composite system with a heterogeneous structure and phase segregation [32]. It can be seen that the Cole–Cole curve of *K* composite, CR composite and all hybrid C:K composite is imperfect semi-circular arcs, represented as a heterogeneous composite structure. However, *K* composite, CR composite and 7C:3 K composite are even imperfect semi-circular, but still represent the arc shape. It is an indication of a better fiber/matrix adhesion as reported by [44]. It is also supported by researchers who claim that the revolution of the system into an elliptical shape implies stronger adhesion between the multiphase components in the polymeric composite system [45]. Additionally, it is noted that composite CR shows a narrower curve shape compared to composite *K*, which appears to

be a wider peak shape. This shows that the type of fiber and interfacial bonding affect the structure of the Cole–Cole curve, which in turn affects the visco-elastic characteristic. In addition, the Cole–Cole curve also reveals the signs of constructive effects of hybridization whereby the hybrid composites on 7C:3 K hybrid composite exhibit comparatively more perfect semi-circular peak forms, while 5C:5 K composite and 3C:7 K composite are extremely imperfect semi-circular and irregular shapes, thus indicating the heterogeneity of the polymeric composite structures. The shape of the Cole–Cole plot is influenced by the proportion and type of fibers, causing the dynamic mechanical properties of CR, *K* and its hybrid composites.

## Flammability

### Underwriters laboratories 94 horizontal burning test (UL 94HB)

UL-94 relates to the 'Standard for Measuring the Flammability of Plastic Products for Components of Equipment and Appliances' issued by Underwriters Laboratories of the United States [46]. In this research, the UL-94 horizontal burning (HB) flammability rating of hybrid natural fiber-reinforced MWCNT-phenolic composites was investigated. The HB test determines the specimen's burning

**Table 6** Data obtained for UL-94 Horizontal and LOI testing for hybrid (C and K) fiber reinforced MWCNT-phenolic composites

| Composites | UL-94 Horizonta/mm min⁻¹ | | | LOI/% | | | | |
|---|---|---|---|---|---|---|---|---|
| | Dripping | Linear burning rate, V/mm min⁻¹ | Rating | $C_F$ | k | d | LOI (vol. %) | Standard deviation |
| 10C:0 K | No | 0 | H-B | 25.7 | −0.94 | 0.2 | 26.31 | 0.18 |
| 7C:3 K | No | 0 | H-B | 27.2 | −1.60 | 0.2 | 26.88 | 0.19 |
| 5C:5 K | No | 0 | H-B | 27.0 | −0.83 | 0.2 | 26.90 | 0.13 |
| 3C:7 K | No | 0 | H-B | 26.8 | −0.83 | 0.2 | 26.97 | 0.11 |
| 0C:10 K | No | 0 | H-B | 27.9 | −0.50 | 0.2 | 27.80 | 0.37 |

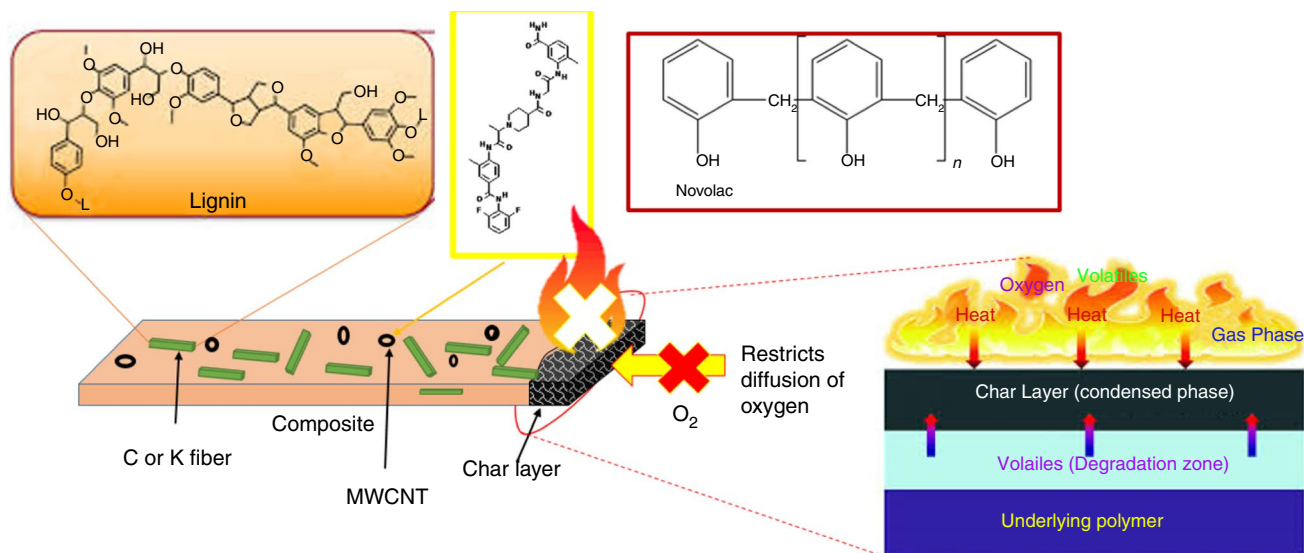Flame is extinguished before the first mark (UL-94 Horizontal)



**Fig. 7** The char formation during the pyrolysis process of the composite

rate in mm min⁻¹ and offers information on the composite materials' ignitability as well as flame distribution characteristics. Table 6 displays the findings and data collected from the UL-94 test. After the flame was removed from all composite specimens, the flame was unable to exceed the 1st gauge mark, resulting in extinguished burning. It implies that all composite materials are in the H-B self-extinguishing ranking and comply with the UL-94 test standard. With the addition of natural fibers to MWCNT-phenolic composites, the flammability of UL-94 horizontal has shown promising results, although natural fibers are highly flammable. The flammability of UL-94 horizontal of MWCNT-phenolic with natural fiber addition indicated promising results, despite the fact that natural fibers are highly flammable.

Flame dripping has not been detected on any set of hybrid phenolic composite, a char layer developed with less smoke. Similar findings were also reported by [47]. The development of a char layer on its surface preserves the internal structure [48]. In addition, char also acts as an isolation layer between the fire and composite surface.

Higher yields of char are beneficial with respect to fire retardation, since char forms an insulation layer as shown in Fig. 7. During the ignition process, the insulation layer inhibits the transfer of heat within the specimen, thereby enhancing the flame's properties [49]. The higher lignin content of the natural fiber, which resulted in the production of the char, enriched the flammability features of the composites [50]. Therefore, all hybrid composites were found to be self-extinguished within 25 s after the flame was extracted without any burning drops.

### Limiting oxygen index (LOI)

The lowest oxygen concentration needed to facilitate flammable combustion of the substance is described by the LOI indices, which are used to describe the flammability of polymeric composite materials. Table 7 shows the LOI results for the C and K fiber hybrid composites. The 10C:0 K composite LOI value is 25.51%. Compared to other composites, it is graded as more readily combustible. The LOI value is also greater than the content of air oxygen of about 21%.

**Table 7** Cone calorimetry data for CR/kenaf reinforced phenolic composites

| Composites | TTI/s | HRR/kW m$^{-2}$ | pHRR/kW m$^{-2}$ | At time/s | THR/MJ m$^s$ | FPI = TTI/PHRR | MLR$_{AVG}$ g/m2s | FIGRA/W m$^{-2}$ s$^{-1}$ | MARHE/kW m$^{-2}$ |
|---|---|---|---|---|---|---|---|---|---|
| 10C:0 K | 61 (2) | 61 (3) | 187 (11) | 176 (2) | 75 (1) | 0.33 | 3.74 (1.2) | 1335 (127) | 111 (4) |
| 7C:3 K | 100 (3) | 40 (2) | 209 (8) | 231 (4) | 74 (2) | 0.51 | 2.21 (1.8) | 1353 (113) | 104 (8) |
| 5C:5 K | 102 (2) | 37 (3) | 215 (8) | 231 (5) | 68 (1) | 0.46 | 2.23 (1.4) | 1219 (142) | 111 (5) |
| 3C:7 K | 162 (4) | 36 (4) | 205 (9) | 222 (3) | 65 (3) | 0.71 | 2.09 (1.2) | 1039 (122) | 83 (4) |
| 0C:10 K | 65 (3) | 59 (3) | 219 (10) | 207 (2) | 76 (2) | 0.30 | 3.55 (1.3) | 1208 (132) | 104 (5) |

The values in parentheses are the standard deviations

TTI = Time to ignition (s), HRR = heat release rate, pHRR = peak heat release rate, at time = Time at peak heat release rate, THR = Total heat release, FPI = fire performance index (ratio of time to ignition (TTI) to PHRR), MLR$_{AVG}$ = average mass loss rate, FIGRA = fire growth rate index, MARHE = maximum average rate of heat emission

Therefore, without an external heat source, the combustion mechanism will not sustain itself at the ambient temperature. The highest LOI value for composites of 0C:10 K was found to be about 27.80%. The incorporation of kenaf fibers thus increases the flame-retardant properties of hybrid composites. The highest LOI value of phenolic composites-based CR fiber meets the Federal Aviation Administration's (FAA) flammability regulations and is a viable replacement material for aviation and automotive interiors. Materials that ranges between 20.95 and 28 of the LOI are known to be 'slow-burning' and marginally stable with self-extinguishing thresholds according to [51]. Therefore, all the composites tested are in the range of slow burning. The kenaf composite has the highest LOI with the most self-extinguishing threshold.

### Cone calorimetry (CC)

Table 7 represents the time to ignition (TTI), heat release rate (HRR), peak heat release rate (pHRR), total heat release rate (THR), fire performance index (FPI), average mass loss rate (MLR$_{AVG}$), fire growth rate index (FIGRA) and maximum average rate of heat emission (MARHE). In an oxygen-regulated setting, as the composite material exposes to constant heat flux, TTI measures the time taken for ignition. It indicates how quickly the specimen's surface achieves the pyrolysis temperature and creates the flammable volatile gasses required to keep the flames on the whole surface of the sample.

The HRR is another critical factor that evaluates the flammability of the material. HRR is represented as the fire intensity by the sum of heat emitted per unit area of the material when it is exposed to fire [52]. Higher TTI and low HRR peaks are often more suitable and are known to be extremely flame-retardant material.

TTI values are increased and HRR values reduced in hybrid fiber compared to the distinct fiber of CR and kenaf. TTI can be affected by the thermal conductivity of the

polymeric matrix and the supply of oxygen concentration and the structure of the composites [15]. In addition, it is reported that the pHRR span for hybrid fiber has also been prolonged. The creation of a defensive carbonaceous layer causes a delay in flame initiation and the establishment of pHRR in hybrid composites. The carbonaceous layer functions as a heat and flame insulator, minimizing the leakage of reactive volatile gases and oxygen diffusion through composites [53].

In contrast to the individual fiber, the fire resistance of hybrid fiber-reinforced composites is higher. Hybrid fiber (CR and *K*)-reinforced composites have been due to the existence of more uniform dispersion and homogeneous mixing of fibers, and the hollowness of the fibers serving as heat flux barriers. Furthermore, the flammability properties of natural fiber composites depend on the fiber type, content and treatment, and fiber dispersion in the composites [52]. Additionally, agglomeration of MWCNTs in a fraction of hybrid fibers causes in composites absorbing more heat through heat radiation, resulting in higher thermal conductivity, which precipitates polymer breakdown.

Figure 8 displays the HRR curve for hybrid composites. Hybrid composites have been found to have two peaks; (1) the first peak refers to the carbonaceous char form in the carbonaceous period, whereas (2) the second peak represents combustion through cracking and oxidizing the char residue. Phenolic, which is highly cross-linked, and casein, bio-based polymer, form a char during combustion [15]. The char layer serves as a protective barrier between the condensed and gaseous phases, limiting mass and volatile transfer. Char acts as a heat barrier between the heat source and the lower polymer layers. A compact char serves as an oxygen and heat insulation barrier [54]. When flammable volatiles come into contact with oxygen, the reactive H and OH radicals are formed to further promote the decomposition and combustion of the polymer composites [15]. As the burning progressed, an abundance of trapped volatiles generated a high

**Fig. 8** Heat release rate curves as function of time for C/K reinforced MWCNT modified phenolic composites
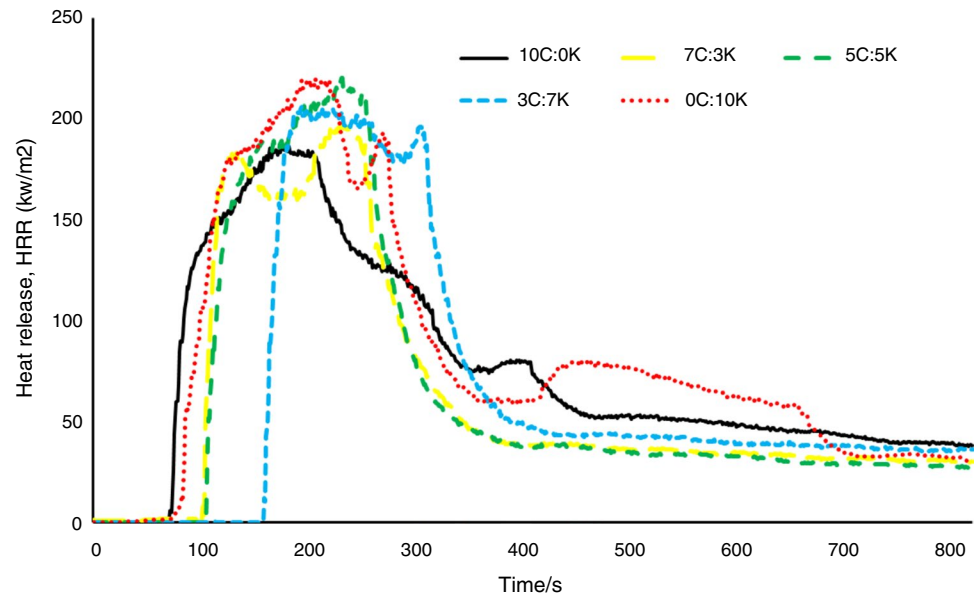


internal pressure during escape, hence enlarging the voids created.

The peak HRR (pHRR) indicates the maximum amount of heat released during combustion, whereas the area underneath the HRR is defined by the THR. Higher pHRR implies a quicker fire development and thus a higher fire risk for these composites. The pHRR of 0C:10 K composite reported the highest value of 219 kW m$^{-2}$, the highest THR value of 76 MJ m$^{-2}$, among other composites. Fire indexes such as the fire growth rate index (FIGRA) and the maximum annual heat emission rate (MAHRE) are adequate criteria to confirm the composite materials' fire retardant properties. The higher the FIGRA value, the quicker the fire spreads and propagates [55]. Meanwhile, MAHRE is regarded as accumulative total heat release divided by time. MAHRE is helpful in rating materials to promote flame spreading to other items [56]. Based on Table 7, 3C:7 K composites recorded the lowest index for FIGRA and MAHRE indicated as the most fire-retardant properties. Mass loss rate (MLR) offers details on physical improvements by composite

deterioration as a yield of char. The reduced average mass loss rate (MLR$_{AVG}$) implies a sluggish burning rate.

The fire performance index (FPI) is measured as the ratio of the TTI to the flashover pattern shown by the pHRR [57]. The higher FPI values could primarily specify a higher fire retardancy efficiency [58]. The lower FPI values are 0.33 and 0.30, respectively, for C-reinforced composite and kenaf-reinforced composite. FPI values are, however, increased for the hybrid fiber and reported as highest as 0.71 for 3C:7 K composites. It is obvious that, among other proportional hybrid composites, with highest TTI and FPI, lowest THR and MLR$_{AVG}$, with lowest FIGRA and MARHE index, 3C:7 K composite reveals the best fire-retardant efficiency. It indicated that kenaf fiber is more flammable compared to C fiber. In fact, lignin is responsible for the volatile–char interactions. It has been reported that the high lignin content of plant promotes carbonization and increases the carbon and ash content of biochar [34]. The content of lignin in CR is 20.70%, while in kenaf is 12.10%, also a contribution on the flammability behavior of the natural fiber. For hybrid

**Table 8** Smoke emission properties of CR/ kenaf reinforced phenolic hybrid composites

| Composites | Dynamic method | | | Static method | |
|---|---|---|---|---|---|
| | Cone calorimeter | | | Smoke density | |
| | TSP/m2 | SMOGRA /m$^2$ s$^{-2}$ | SEA/$_{AVG}$ m$^2$ kg$^{-1}$ | D$_{s,max}$ | VOF4 |
| 10C:0K | 3.6 (0.6) | 1.39 (0.7) | 38.09 (3.8) | 284.24 (22.1) | 48.15 (9.6) |
| 7C:3K | 3.7 (0.6) | 1.44 (0.8) | 30.73 (4.1) | 348.03 (40.4) | 35.59 (5.2) |
| 5C:5K | 3.9 (0.4) | 1.57 (0.6) | 32.79 (2.8) | 270.90 (32.9) | 28.26 (7.5) |
| 3C:7K | 4.5 (0.8) | 1.58 (0.9) | 33.92 (3.5) | 315.05 (28.7) | 18.76 (4.2) |
| 0C:10K | 3.1 (0.3) | 1.52 (0.9) | 24.66 (3.6) | 250. 20 (34.8) | 12.34 (3.9) |

$^a$The values in parentheses are the standard deviations

**Table 9** Decision matrix

|  | TGA | Storage Modulus | LOI | FPI | VOF |
|---|---|---|---|---|---|
| 10C:0 K | 32.07 | 3470 | 26.31 | 0.33 | 48.15 |
| 7C:3 K | 32.46 | 4180 | 26.88 | 0.51 | 35.59 |
| 5C:5 K | 22.8 | 2470 | 26.9 | 0.46 | 28.26 |
| 3C:7 K | 31.59 | 3370 | 26.97 | 0.71 | 18.76 |
| 0C:10 K | 30.09 | 5740 | 27.8 | 0.3 | 12.34 |

**Table 10** The normalized matrix

|  | TGA | Storage Modulus | LOI | FPI | VOF |
|---|---|---|---|---|---|
| 10C:0 K | 0.478 | 0.388 | 0.425 | 0.304 | 0.689 |
| 7C:3 K | 0.484 | 0.468 | 0.448 | 0.471 | 0.509 |
| 5C:5 K | 0.34 | 0.276 | 0.449 | 0.424 | 0.404 |
| 3C:7 K | 0.471 | 0.377 | 0.45 | 0.655 | 0.268 |
| 0C:10 K | 0.448 | 0.642 | 0.464 | 0.277 | 0.177 |

**Table 11** The weighted normalized matrix

|  | TGA | Storage Modulus | LOI | FPI | VOF |
|---|---|---|---|---|---|
| 10C:0 K | 0.096 | 0.078 | 0.085 | 0.061 | 0.138 |
| 7C:3 K | 0.097 | 0.094 | 0.09 | 0.094 | 0.102 |
| 5C:5 K | 0.068 | 0.055 | 0.09 | 0.085 | 0.081 |
| 3C:7 K | 0.094 | 0.075 | 0.09 | 0.131 | 0.054 |
| 0C:10 K | 0.09 | 0.128 | 0.093 | 0.055 | 0.035 |

**Table 12** The positive and negative ideal values

|  | Positive ideal | Negative ideal |
|---|---|---|
| TGA | 0.097 | 0.068 |
| Storage Modulus | 0.128 | 0.055 |
| LOI | 0.093 | 0.085 |
| FPI | 0.131 | 0.055 |
| VOF | 0.035 | 0.138 |

**Table 13** Distance to positive, negative ideal points and the relative closeness value and ranking

| Composites | Distance to positive and negative ideal points | | The relative closeness value and ranking | |
|---|---|---|---|---|
|  | Distance to positive ideal | Distance to negative ideal | Relative closeness, $C_i$ | Rank |
| 10C:0 K | 0.134 | 0.036 | 0.211 | 5 |
| 7C:3 K | 0.084 | 0.071 | 0.46 | 3 |
| 5C:5 K | 0.102 | 0.064 | 0.387 | 4 |
| 3C:7 K | 0.056 | 0.118 | 0.677 | 1 |
| 0C:10 K | 0.076 | 0.128 | 0.627 | 2 |

composites, a substantial reduction in pHRR between 2 and 15% and THR between 2 and 13% was observed. The lower pHRR and THR in hybrid composites as compared to kenaf-reinforced composites are attributable to char augmentation, which promotes thermal stability.

**Smoke density**

The emission of smoke, which is a gaseous phase and the materials of incomplete combustion, is a state of combustion. A single-chamber test (static method) and a cone calorimetry test (dynamic method) were used for heat emission testing. In the dynamic method, with additional gas motions, smoke moves through the measurement area, whereas in the static method, smoke accumulates in the closed chamber [59]. Table 8 presents the smoke emissions of the composites. Total smoke production (TSP) and smoke growth rate index (SMOGRA) are the factors used to measure the volume of smoke emitted. These parameters are commonly accepted by the Euroclass system in 'Single Burning Object Test EN 13,823' [53]. A better smoke suppression property shown by kenaf-reinforced phenolic composites followed by CR-reinforced phenolic composites was found. The lowest TSP value observed for kenaf-reinforced phenolic composites followed by CR-reinforced phenolic composites. Hybrid composites, however, released more TSPs than distinct fiber composites. The lowest SMOGRA value observed for CR-reinforced phenolic composites followed by kenaf-reinforced phenolic composites. Hybrid composites emitted more SMOGRA than distinct fiber composites.

The composite burning behaviors are largely defined by the matrix properties and the reinforcement of fibers and by any synergistic or antagonistic effects, and the composite flame retardancy [15]. The average smoke extinction area ($SEA_{AVG}$) is a factor that corresponds to the absorption of light by the surface of smoke particles produced during combustion. In addition, the properties of the smoke intensity, namely the maximum value of the specific optical density (Ds, max) and the cumulative value of the specific optical smoke density for the first 4 min (VOF), are shown in Table 9. Smoke gases are collected during the test period, thus reducing the transmission of light and thereby increasing the Ds and VOF. The result indicated that the smoke concentration of CR-reinforced phenolic composites is higher than kenaf-reinforced phenolic composites. The behavior of CR-reinforced phenolic composites is ignited earlier and extinguished later. This usually results in a higher amount of TSP, as confirmed by the total smoke production

**Fig. 9** Relative closeness factor of C and/ or K hybrid modified phenolic composite
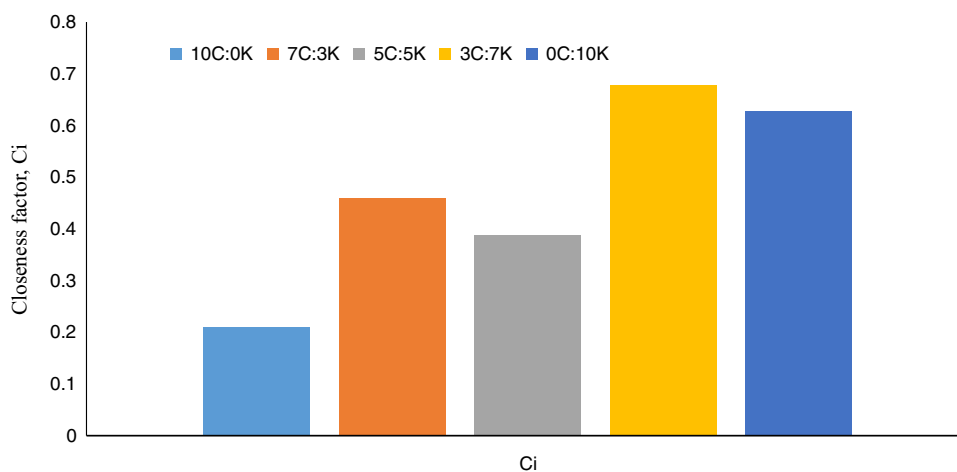


Thermal properties ranking of C and/or K hybrid modified phenolic compsites

data provided in Table 10. The lower smoke production of composites reinforced by kenaf is due to the greater ability of this phenolic to form char with proportional kenaf. Smoke density of all the hybrid composites is found to be less than 200 where complied with the requirement of Federal Aviation Regulations (FAR) 25.853d, on specific optical density of smoke generated by interior materials of aircraft; smoke density (Ds) in 4 min is $< = 200$ [60]. The incorporation of CR into phenolic exhibited significant improvement on the fire-retardant behavior. Nonetheless, there is no significant improvement on smoke suppression.

## TOPSIS method

The best properties of hybrid composite for potential applications have been selected and ranked by the TOPSIS method. The decision matrix, normalization matrix, mass-normalized matrix, positive and negative ideal values, distance to positive and negative ideal points, relative closeness value known as $c_i$ value and ranking are shown in Tables 9–13. Table 9 depicts the decision matrix, whereas Table 10 depicts the normalized matrix. The weighted normalized decision matrix, as well as the positive and negative ideal values, is shown in Tables 11 and 12. Table 13 represents the distance to the positive and negative ideal solutions, and the relative closeness degree of each alternative to the ideal solution.

Finally, the ranking of thermal properties of hybrid composite based on their proportion and properties is shown in Fig. 9. According to the findings, the optimal hybrid proportion of CR and kenaf fiber phenolic composite was 3C:7 K composite, which had a relative closeness to the ideal solution and values of 0.677. It has been noticed that composite materials are ranked as follows: Rank 1 (3C:7 K), Rank 2 (0C:10 K), Rank 3 (7C:3 K), Rank 4 (5C:5 K) and Rank

5 (10C:0 K). The TOPSIS approach was found to be the most effective method for selecting the optimal proportion of hybrid composites from a set of composites [61].

## Conclusions

Based on TGA, DTG and DSC curve, 7C:3 K composites exhibited the highest thermal stability among the composite samples. The addition of K in CR composites (7C:3 K) led to the highest storage modulus, the $T_g$ value, compared to CR composites. The high $T_g$ values correlated to a decrease in molecular movement of matrix with addition of fiber, indicating a strong interfacial bonding between fiber and matrix. After flame removal, all composite materials have extinguished combustion, are in the H-B self-extinguishing rating and comply with the UL-94 test standard. The addition of highly flammable natural fibers to modified phenolic composites has shown promising UL-94 horizontal results. All the composites tested for LOI are in the range of 26–28. These are considered as slow burning and the kenaf composite has the highest LOI with the most self-extinguishing threshold. Among other proportional hybrid composites, with highest TTI and FPI, lowest THR and $MLR_{AVG}$, with lowest FIGRA and MARHE index, 3C:7 K composite possessed the best fire-retardant efficiency. The smoke density of all the hybrid composites was found to be less than 200 which complied with the requirement of FAR 25.853d. Based on the TOPSIS approach, 3C:7 K composite was selected as the best hybrid ratio between CR and kenaf fiber phenolic composite for high-temperature structural applications.

## Declarations

**Conflict of interest** The authors declare no conflicts of interest.

# References

1. Aliotta L, Gigante V, Coltelli MB, Cinelli P, Lazzeri A. Evaluation of Mechanical and Interfacial Properties of Bio-Composites Based on Poly(Lactic Acid) with Natural Cellulose Fibers. Int J Mol Sci. 2019;20(4):960.

2. Jawaid M, Abdul Khalil HPS, Hassan A, Dungani R, Hadiyane A. Effect of jute fibre loading on tensile and dynamic mechanical properties of oil palm epoxy composites. Compos B Eng. 2013;45(1):619–24. https://doi.org/10.1016/j.compositesb.2012.04.068.

3. Shanmugam V, Mensah RA, Försth M, Sas G, Restás Á, Addy C, et al. Circular economy in biocomposite development: State-of-the-art, challenges and emerging trends. Compos Part C: Open Access. 2021;5:100138.

4. Luhar S, Suntharalingam T, Navaratnam S, Luhar I, Thamboo J, Poologanathan K, et al. Sustainable and renewable bio-based natural fibres and its application for 3D printed concrete: a review. Sustainability. 2020;12(24):10485.

5. Loganathan TM, Sultan MTH, Ahsan Q, Jawaid M, Naveen J, Shah AUM, et al. Characterization of alkali treated new cellulosic fibre from Cyrtostachys renda. J Market Res. 2020;9(3):3537–46.

6. Ramesh M. Kenaf (Hibiscus cannabinus L) fibre based bio-materials: a review on processing and properties. Progress Mater Sci. 2016;78:1–92.

7. Asim M, Jawaid M, Paridah MT, Saba N, Nasir M, Shahroze RM. Dynamic and thermo-mechanical properties of hybridized kenaf/PALF reinforced phenolic composites. Polym Compos. 2019;40(10):3814–22. https://doi.org/10.1002/pc.25240.

8. Hanan F, Jawaid M, Tahir PM. Mechanical performance of oil palm/kenaf fiber-reinforced epoxy-based bilayer hybrid composites. J Nat Fibers. 2018;17:155.

9. Khoshnava SM, Rostami R, Ismail M, Rahmat AR, Ogunbode BE. Woven hybrid Biocomposite: Mechanical properties of woven kenaf bast fibre/oil palm empty fruit bunches hybrid reinforced poly hydroxybutyrate biocomposite as non-structural building materials. Constr Build Mater. 2017;154:155–66.

10. Abdullah S, Zuhudi N, Anuar N, Isa M, editors. Mechanical and thermal characterization of alkali treated kenaf fibers. IOP Conference Series: Materials Science and Engineering; 2018: IOP Publishing.

11. Monteiro SN, Calado V, Rodriguez RJS, Margem FM. Thermogravimetric behavior of natural fibers reinforced polymer composites—an overview. Mater Sci Eng, A. 2012;557:17–28.

12. Joseph S, Appukuttan SP, Kenny JM, Puglia D, Thomas S, Joseph K. Dynamic mechanical properties of oil palm microfibril-reinforced natural rubber composites. J Appl Polym Sci. 2010;117(3):1298–308.

13. Frollini E, Silva C, Ramires E. Phenolic resins as a matrix material in advanced fiber-reinforced polymer (FRP) composites. Advanced fibre-reinforced polymer (FRP) composites for structural applications. Elsevier; 2013. p. 7–43.

14. Asim M, Saba N, Jawaid M, Nasir M, Pervaiz M, Alothman OY. A review on phenolic resin and its composites. Curr Anal Chem. 2018;14(3):185–97.

15. Chapple S, Anandjiwala R. Flammability of natural fiber-reinforced composites and strategies for fire retardancy: a review. J Thermoplast Compos Mater. 2010;23(6):871–93.

16. Naveen J, Muthukumar C, Jawaid M. Thermal Properties of Phenolic Composites. Phenolic Polymers Based Composite Materials. Springer; 2020. p. 191–205.

17. Asim M, Jawaid M, Nasir M, Saba N. Effect of fiber loadings and treatment on dynamic mechanical, thermal and flammability properties of pineapple leaf fiber and kenaf phenolic composites. J Renew Mater. 2018;6(4):383–93.

18. Asim M, Paridah M, Saba N, Jawaid M, Alothman OY, Nasir M, et al. Thermal, physical properties and flammability of silane treated kenaf/pineapple leaf fibres phenolic hybrid composites. Compos Struct. 2018;202:1330–8.

19. Mathur R, Singh B, Dhami T, Kalra Y, Lal N, Rao R, et al. Influence of carbon nanotube dispersion on the mechanical properties of phenolic resin composites. Polym Compos. 2010;31(2):321–7.

20. Eslami Z, Yazdani F, Mirzapour MA. Thermal and mechanical properties of phenolic-based composites reinforced by carbon fibres and multiwall carbon nanotubes. Compos A Appl Sci Manuf. 2015;72:22–31.

21. Allcorn EK, Natali M, Koo JH. Ablation performance and characterization of thermoplastic polyurethane elastomer nanocomposites. Compos A Appl Sci Manuf. 2013;45:109–18.

22. Park J-M, Kwon D-J, Wang Z-J, Roh J-U, Lee W-I, Park J-K, et al. Effects of carbon nanotubes and carbon fiber reinforcements on thermal conductivity and ablation properties of carbon/phenolic composites. Compos B Eng. 2014;67:22–9.

23. Li Q, Chen L, Li X, Zhang J, Zhang X, Zheng K, et al. Effect of multi-walled carbon nanotubes on mechanical, thermal and electrical properties of phenolic foam via in-situ polymerization. Compos A Appl Sci Manuf. 2016;82:214–25.

24. Loganathan; TM, Sultan; MTH, Jawaid; M, Ahsan; Q, Naveen; J, Shah; AUM et al. Physical, mechanical and morphological properties of hybrid Cytostachys Renda /kenaf fiber reinforced with Multi-Walled Carbon Nanotubes (MWCNT)-phenolic composites. Polymers. 2021. In press.

25. Jesuarockiam N, Jawaid M, Zainudin ES, Thariq Hameed Sultan M, Yahaya R. Enhanced thermal and dynamic mechanical properties of synthetic/natural hybrid composites with graphene nanoplateletes. Polymers. 2019;11(7):1085.

26. Di Gregorio L, Ronchetti S, Onida B. Phenolic resin emissions upon thermal degradation. Eurobrake; 2015.

27. Jiang H, Wang J, Wu S, Yuan Z, Hu Z, Wu R, et al. The pyrolysis mechanism of phenol formaldehyde resin. Polym Degrad Stab. 2012;97(8):1527–33.

28. Mahajan A, Kingon A, Kukovecz A, Konya Z, Vilarinho PM. Studies on the thermal decomposition of multiwall carbon nanotubes under different atmospheres. Mater Lett. 2013;90:165–8.

29. Safri SNA, Sultan MTH, Shah AUM. Characterization of benzoyl treated sugar palm/glass fibre hybrid composites. J Market Res. 2020;9(5):11563–73.

30. Asim M, Jawaid M, Khan A, Asiri AM, Malik MA. Effects of Date Palm fibres loading on mechanical, and thermal properties of Date Palm reinforced phenolic composites. J Market Res. 2020;9(3):3614–21. https://doi.org/10.1016/j.jmrt.2020.01.099.

31. Prime RB. Dynamic mechanical analysis of thermosetting materials. 2005.

32. Naveen J, Jawaid M, Zainudin E, Sultan MT, Yahaya R, Majid MA. Thermal degradation and viscoelastic properties of Kevlar/Cocos nucifera sheath reinforced epoxy hybrid composites. Compos Struct. 2019;219:194–202.

33. Safri SNA, Sultan MTH, Jawaid M, Majid MA. Analysis of dynamic mechanical, low-velocity impact and compression after impact behaviour of benzoyl treated sugar palm/glass/epoxy composites. Compos Struct. 2019;226:111308.

34. Saba N, Paridah M, Abdan K, Ibrahim NA. Dynamic mechanical properties of oil palm nano filler/kenaf/epoxy hybrid nanocomposites. Constr Build Mater. 2016;124:133–8.

35. Saha P, Chowdhury S, Roy D, Adhikari B, Kim JK, Thomas S. A brief review on the chemical modifications of lignocellulosic fibers for durable engineering composites. Polym Bull. 2016;73(2):587–620. https://doi.org/10.1007/s00289-015-1489-y.

36. Pothan LA, Thomas S, Groeninckx G. The role of fibre/matrix interactions on the dynamic mechanical properties of chemically modified banana fibre/polyester composites. Compos A Appl Sci Manuf. 2006;37(9):1260–9.

37. Ornaghi HL Jr, Bolner AS, Fiorio R, Zattera AJ, Amico SC. Mechanical and dynamic mechanical analysis of hybrid composites molded by resin transfer molding. J Appl Polym Sci. 2010;118(2):887–96.

38. Romanzini D, Ornaghi HL Jr, Amico SC, Zattera AJ. Influence of fiber hybridization on the dynamic mechanical properties of glass/ramie fiber-reinforced polyester composites. J Reinf Plast Compos. 2012;31(23):1652–61.

39. Chee SS, Jawaid M, Sultan MT. Thermal stability and dynamic mechanical properties of kenaf/bamboo fibre reinforced epoxy composites. BioResources. 2017;12(4):7118–32.

40. Nurazzi NM, Khalina A, Sapuan SM, Ilyas RA, Rafiqah SA, Hanafee ZM. Thermal properties of treated sugar palm yarn/glass fiber reinforced unsaturated polyester hybrid composites. J Market Res. 2020;9(2):1606–18. https://doi.org/10.1016/j.jmrt.2019.11.086.

41. Abu-Abdeen M. Static and dynamic mechanical properties of poly (vinyl chloride) loaded with aluminum oxide nanopowder. Mater Des. 2012;33:523–8.

42. Tang X, Yan X. A review on the damping properties of fiber reinforced polymer composites. J Ind Text. 2020;49(6):693–721.

43. Mohammed BR, Leman Z, Jawaid M, Ghazali MJ, Ishak MR. Dynamic mechanical analysis of treated and untreated sugar palm fibre-based phenolic composites. BioResources. 2017;12(2):3448–62.

44. Chee SS, Jawaid M, Sultan MTH, Alothman OY, Abdullah LC. Thermomechanical and dynamic mechanical properties of bamboo/woven kenaf mat reinforced epoxy hybrid composites. Compos B Eng. 2019;163:165–74. https://doi.org/10.1016/j.compositesb.2018.11.039.

45. Panwar V, Pal K. An optimal reduction technique for rGO/ABS composites having high-end dynamic properties based on Cole-Cole plot, degree of entanglement and C-factor. Compos B Eng. 2017;114:46–57.

46. Mngomezulu ME, John MJ, Jacobs V, Luyt AS. Review on flammability of biofibres and biocomposites. Carbohyd Polym. 2014;111:149–82.

47. Liu J, Wang L, Zhang W, Han Y. Phenolic Resin Foam Composites Reinforced by Acetylated Poplar Fiber with High Mechanical Properties, Low Pulverization Ratio, and Good Thermal Insulation and Flame Retardant Performance. Materials. 2020;13(1):148.

48. Hidalgo JP, Torero JL, Welch S. Fire performance of charring closed-cell polymeric insulation materials: Polyisocyanurate and phenolic foam. Fire Mater. 2018;42(4):358–73.

49. Auad ML, Zhao L, Shen H, Nutt SR, Sorathia U. Flammability properties and mechanical performance of epoxy modified phenolic foams. J Appl Polym Sci. 2007;104(3):1399–407.

50. Friedrich K, Breuer U. Multifunctionality of polymer composites: challenges and new solutions. Norwich: William Andrew; 2015.

51. Fenimore CP. Candle-type test for flammability of polymers. Flame-retardant polymeric materials. Springer; 1975. p. 371–97.

52. Mochane M, Mokhena TC, Mokhothu T, Mtibe A, Sadiku E, Ray SS et al. Recent progress on natural fiber hybrid composites for advanced applications: a review. 2019;13(2):159–198.

53. Chee SS, Jawaid M, Alothman OY, Yahaya R. Thermo-oxidative stability and flammability properties of bamboo/kenaf/nanoclay/epoxy hybrid nanocomposites. RSC Adv. 2020;10(37):21686–97.

54. Levința N, Vuluga Z, Teodorescu M, Corobea MC. Halogen-free flame retardants for application in thermoplastics based on condensation polymers. SN Appl Sci. 2019;1(5):422. https://doi.org/10.1007/s42452-019-0431-6.

55. Liu T, Jing J, Zhang Y, Fang Z. Synthesis of a novel polyphosphate and its application with APP in flame retardant PLA. RSC Adv. 2018;8(8):4483–93.

56. Morgan AB, Gagliardi NA, Price WA, Galaska ML. Cone calorimeter testing of S2 glass reinforced polymer composites. Fire Mater: Int J. 2009;33(7):323–44.

57. Vahabi H, Kandola BK, Saeb MR. Flame retardancy index for thermoplastic composites. Polymers. 2019;11(3):407.

58. Realinho V, Haurie L, Antunes M, Velasco JI. Thermal stability and fire behaviour of flame retardant high density rigid foams based on hydromagnesite-filled polypropylene composites. Compos B Eng. 2014;58:553–8. https://doi.org/10.1016/j.compositesb.2013.11.015.

59. Sałasińska K, Borucka M, Celiński M, Gajek A, Zatorski W, Mizera K, et al. Thermal stability, fire behavior, and fumes emission of polyethylene nanocomposites with halogen-free fire retardants. Adv Polym Technol. 2018;37(7):2394–410.

60. Techinal brief: Kydex thermoplastics In: FAR 25.853a and FAR 25.853d. Sekisui Spi, Curbell Plastics Accessed 22/02/2021 2021.

61. Sanjay M, Jawaid M, Naidu N, Yogesha B. TOPSIS method for selection of best composite laminate. Modelling of Damage Processes in Biocomposites, Fibre-Reinforced Composites and Hybrid Composites. Elsevier; 2019. p. 199–209.